Quantum weak torque sensing with squeezed optomechanics

Jie Wang, Qian Zhang, and Hui Jing*

Key Laboratory of Low-Dimensional Quantum Structures and Quantum Control of Ministry of Education, Department of Physics and Synergetic Innovation Center for Quantum Effects and Applications, Hunan Normal University, Changsha 410081, China

(Received 27 June 2024; accepted 20 August 2024; published 3 September 2024)

Quantum-enhanced cavity optomechanical (COM) sensors, utilizing quantum resources, have become powerful tools for precisely measuring a wide range of physical quantities, from gravitational waves to accelerations. However, quantum-enhanced COM torque sensing remains an area of exploration. In this work, we show that utilizing quantum squeezing can suppress the quantum noise of a COM torque sensor below the standard quantum limit. We theoretically predict that our COM torque sensor can achieve an approximately 20-dB quantum advantage by optimizing the homodyne detection. Our approach is compatible with available engineering techniques of advanced COM sensors, with potential applications ranging from nanoscale magnetism to the quantum geometric phase.

DOI: 10.1103/PhysRevA.110.033505

I. INTRODUCTION

Measurements of mechanical torque or rotation are fundamental to many technological and scientific advancements, from sensitive angular momentum [1,2] and the Casimir effect [3–5] to proposed probes of gravity [6,7] and studies in magnetometry [8–10]. In recent years, cavity optomechanical (COM) systems featuring efficient interactions between light and matter have enabled the detection of diverse physical quantities with enhanced sensitivity [11–15]. It is also possible to utilize COM systems to measure the tiny displacements related to torsional mechanical resonators [16–18]. Recent publications have proposed that COM torque sensors enable advances in applications such as torque magnetometry [19,20], electron spin detection [21], and orbital angular momentum measurement [22,23].

Quantum-enhanced sensors, leveraging unique quantum resources such as quantum entanglement or squeezing, are expected to perform high-precision measurements for various physical quantities [25,26], including weak forces, tiny displacements [27–31], and electromagnetic fields [32–34], to name a few. Recently, rapid advances in COM systems in the deep quantum regime have paved the way for the development of highly flexible and powerful quantum sensors for precise measurements [12,35–38]. The sensitivity of optomechanical sensing is typically constrained by the standard quantum limit (SQL), resulting from the optimal balance between two quantum noise sources, including shot noise and backaction noise [28,39]. Advanced techniques utilizing nonclassical light [26,40], *in situ* imprecision-backaction correlation [28,41,42], and quantum nondemolition or backaction-evading measurements [43–45] have been proposed to reduce quantum noise below the SQL and enhance the measurement sensitivity of COM sensors. Recently, an impressive experiment demonstrated sub-SQL displacement measurement in a COM system with a macroscopic 40-kg mirror by injecting squeezed light [41]. However, the achievement of sub-SQL torque sensing based on COM systems by exploiting the merit of quantum squeezing remains an area of exploration.

In this work, we theoretically demonstrate that using quantum squeezing can lead to significant improvement in COM torque sensor performance. By adjusting the. Optical parametric amplifier (OPA) parameters, the effect of quantum backaction noise can be mitigated, leading to considerable suppression of quantum noise. Further optimization of the homodyne angle can reduce quantum noise to 3 orders of magnitude below the SQL. The scheme we propose, compatible with advanced techniques for fabricating and engineering COM torque sensors, aims to inspire further efforts by integrating more concepts from COM engineering and quantum metrology.

II. SQUEEZING-ENHANCED COM TORQUE SENSING

Research on torsion optics, which focuses on the transfer of angular momentum from light to matter, has been an active field of study since 1935 [2]. With the development of COM devices with torsion pendulums, electron spin [21], photon-shuttling effect [46], optical torque [16,17,47], magnetic moment [19,20], and photon spin angular momentum [22,23] have been successfully realized measurements. We note that, very recently, the key roles of squeezing have also been shown in, e.g., enhancing light-matter interactions [37,38,48–50], protecting quantum states [51–54], and inducing optical nonreciprocity [55,56]. Hence, it is reasonable to investigate quantum torque sensing using a squeezed optomechanical system.

As illustrated in Fig. 1, the COM system under consideration comprises two helical elements: an input coupler that is rigidly fixed and a rear mirror that behaves as a torsional pendulum, oscillating at an angular frequency Ω_ϕ. We suppose

*Contact author: jinghui73@foxmail.com

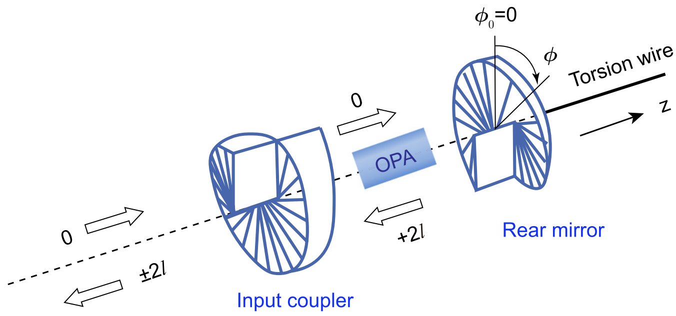

Symbol	Parameter	Value
$\Omega_\phi/2\pi$	Rotating mirror angular frequency	10 MHz
$\kappa/2\pi$	Cavity decay rate	10 MHz
m	Rotating mirror mass	100 ng
l	Orbital angular momentum	100 $\hbar$
Q_ϕ	Mechanical quality factor	2×10^6
$\omega_c/2\pi$	Cavity resonance frequency	10^{14} Hz
R	Rotating mirror Radius	10 μm
λ	Laser wavelength	810 nm
L	Cavity length	1 mm
P_{in}	Input laser power	50 mW

FIG. 1. The cavity comprises a fixed, partially transparent input coupler (static helical element) and a movable, perfectly reflecting rear mirror (oscillating helical mirror). The input coupler preserves the orbital state upon transmission, while it removes $2l$ orbital angular momentum per photon along the z axis upon reflection. Similarly, the reflection on the rear mirror adds $2l$ orbital angular momentum per photon along the z axis. ϕ indicates the angular deflection of the rear mirror from its equilibrium ($\phi_0 = 0$). The nonlinear medium induces intracavity squeezing. We also provide definitions and approximate values of the parameters used in the main text [24].

the rear mirror has a mass m and a radius R, with a moment of inertia about the z axis passing through its center given by $I = mR^2/2$ [2]. The angle ϕ represents the angular deviation of the rear mirror from its equilibrium position ($\phi_0 = 0$) [2,57]. Additionally, the system integrates a nonlinear $\chi^{(2)}$ medium to generate the intracavity squeezing. The Hamiltonian of our COM system in the frame rotating then can be written as [24,58,59]

$$\hat{H} = \hat{\mathcal{H}}_c + \frac{\hbar\Omega_{\hat{\phi}}}{2}(\hat{L}_z^2 + \hat{\phi}^2) + \hbar g_0 \hat{a}^\dagger \hat{a}\hat{\phi},$$
$$\hat{\mathcal{H}}_c = \hbar\Delta_c \hat{a}^\dagger\hat{a} + i\hbar G(e^{i\theta}\hat{a}^{\dagger 2} - e^{-i\theta}\hat{a}^2) + i\hbar\varepsilon(\hat{a}^\dagger - \hat{a}), \quad (1)$$

where $\hat{a}$ and $\hat{a}^\dagger$ denote the bosonic annihilation and creation operators for the cavity mode, respectively. $\Delta_c = \omega_0 - \omega_l$ is the detuning between the cavity field and the driving field. The COM coupling strength is $g_0 = cl(\hbar/I\Omega_\phi)^{1/2}/L$, where c is the speed of light, L is the length of the cavity, and the orbital angular momentum is l. The parameter ε represents the strength of the driving field, while θ and G denote the parametric phase and parametric gain of the nonlinear medium, respectively; $\hat{L}_z$ ($\hat{\phi}$) represents the dimensionless angular momentum (position) operator of the rear mirror, satisfying the commutation relation $[\hat{L}_z, \hat{\phi}] = -i\hbar$ [24,58]. The parameter values used in this work are shown in Fig. 1. The total optical decay rate is $\kappa/2\pi = 10$ MHz, which includes both the decay rate $\kappa_{\rm ex}$ at the input coupler and the intracavity decay rate κ_0. Here, the "efficiency" η_c is defined as $\eta_c = \kappa_{\rm ex}/(\kappa_0 + \kappa_{\rm ex})$. The mechanical quality factor is $Q_\phi = 2\times10^6$, with the angular frequency $\Omega_\phi/2\pi = 10$ MHz. The effective mass is $m = 100$ ng. We define the associated mechanical decay rate as $\Gamma_\tau = D_\phi/I$, where D_ϕ is the intrinsic damping constant of the rear mirror [11]. In practical applications, phase fluctuations of the driving laser may affect quantum phenomena in optomechanical systems [60–62]. Recent studies, however, have explored various methods to suppress the effects of laser phase noise, including destructive interference [63], parametric amplification [64–66], squeezed injection at lower pump power [67], and fiber-loop delay line interferometers [68], to name a few. Hence, at least in principle, the impacts of laser phase noise can be effectively avoided by incorporating these techniques into COM sensing devices. Consequently, the effects of laser phase noise are excluded in the subsequent analysis.

After introducing various dissipations and associated input noise, we can express the quantum Langevin equations as follows:

$$\dot{\hat{\phi}} = \Omega_\phi \hat{L}_z,$$
$$\dot{\hat{L}}_z = -\Omega_\phi\hat{\phi} - \Gamma_\tau\hat{L}_z - g_0\hat{a}^\dagger\hat{a} + \sqrt{2\Gamma_\tau}\hat{\tau}_{\rm in},$$
$$\dot{\hat{a}} = -\left[i\Delta_c + \frac{\kappa}{2}\right]\hat{a} - ig_0\hat{a}\hat{\phi} + 2Ge^{i\theta}\hat{a}^\dagger + \varepsilon + \sqrt{\eta_c\kappa}\hat{a}_{\rm in} + \sqrt{(1-\eta_c)\kappa}\hat{a}_0. \quad (2)$$

The noise operators $\hat{a}^{\rm in}$ and $\hat{a}^0$ represent the noise associated with the input coupler and internal losses, respectively. The noise acting on the rear mirror is $\hat{\tau}_{\rm in} = \hat{\tau}_{\rm th} + \hat{\tau}_{\rm sig}$, where $\hat{\tau}_{\rm th}$ and $\hat{\tau}_{\rm sig}$ represent the scaled thermal torque and the measured torque signal with dimension $\mathrm{Hz}^{1/2}$ [21,69], respectively. All of the noise operators have zero mean values. After straightforward algebraic calculations, we find that $g_0 \ll \{\kappa, \Omega_\phi\}$ and $|\varepsilon| \gg 1$, indicating that our system satisfies the conditions of strong driving and weak optomechanical coupling. Considering strong optical driving, each operator can be expanded as the sum of its classical steady-state mean value and a small quantum fluctuation around it [11], i.e., $\hat{a} = \alpha + \delta\hat{a}$, $\hat{\phi} = \bar{\phi} + \delta\hat{\phi}$, and $\hat{L}_z = \bar{L}_z + \delta\hat{L}_z$. The solutions of the steady-state mean values can be obtained as

$$|\alpha| = \left|\frac{\varepsilon}{\kappa^2/4 + \Delta^2 - 4G^2}\right|\sigma,$$
$$\bar{\phi} = -g_0|\alpha|^2/\Omega_\phi,$$
$$\bar{L}_z = 0, \quad (3)$$

where $\sigma = \sqrt{\kappa^2/4 + \Delta^2 + 4G^2 + 2G(\kappa\cos\theta - 2\Delta\sin\theta)}$, the effective optical detuning is $\Delta = \Delta_c - g_0\bar{\phi}$, and the phase of the intracavity field is $\psi = \arctan[4G\sin\theta - 2\Delta/(4G\cos\theta + \kappa)]$. The "position" and "momentum"-like operators of optical quadrature fluctuations are defined as $\delta\hat{q} = (\delta\hat{a}^\dagger + \delta\hat{a})/\sqrt{2}$ and $\delta\hat{p} = i(\delta\hat{a}^\dagger - \delta\hat{a})/\sqrt{2}$, with the associated optical noise

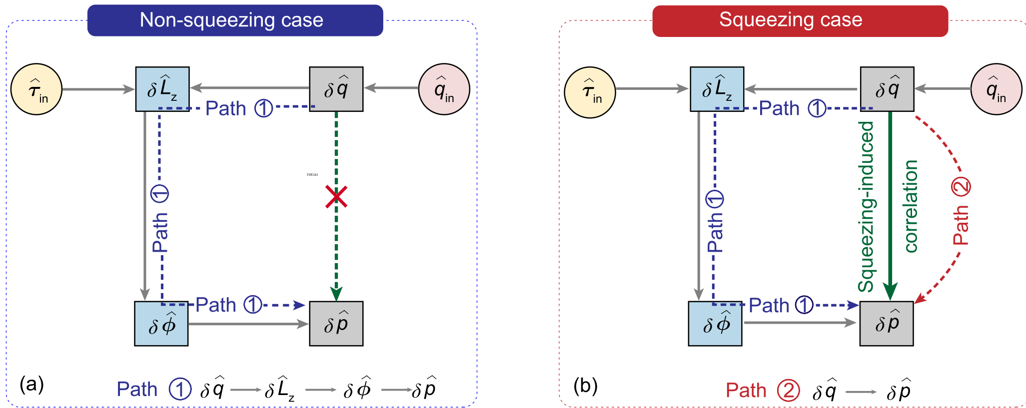

FIG. 2. Quantum backaction noise flowchart. Path ① (blue) illustrates the backaction noise arising from the optomechanical interaction. By utilizing the nonlinear media, it is possible to introduce another path of backaction noise (red). The effects of backaction noise can be effectively mitigated through the destructive interference between Path ① and Path ②, resulting in improved torque sensing sensitivity.

operators $\hat{q}^{\text{in},0}$ ($\hat{p}^{\text{in},0}$) and corresponding correlation functions

$$\langle\delta\hat{q}_u[t]\delta\hat{q}_u[t']\rangle = \langle\delta\hat{p}_u[t]\delta\hat{p}_u[t']\rangle = \frac{1}{2}\delta(t-t'),$$
$$\langle\delta\hat{q}_u[t]\delta\hat{p}_u[t']\rangle = -\langle\delta\hat{p}_u[t]\delta\hat{q}_u[t']\rangle = \frac{\mathrm{i}}{2}\delta(t-t'),$$
$$\langle\hat{\tau}_{\text{th}}[t]\hat{\tau}_{\text{th}}[t']\rangle \simeq \bar{n}_m\delta(t-t'), \quad \text{for } \bar{n}_m, Q_\phi \gg 1, \tag{4}$$

where $u = \text{in}$ and 0, $\bar{n}_m = [\exp(\hbar\Omega_\phi/k_B T) - 1]^{-1}$, and k_{B} and T are the Boltzmann constant and the bath temperature [70], respectively. Then, we can obtain the linearized QLEs describing the quadrature fluctuations [71]

$$\delta\dot{\hat{q}} = (-\kappa/2 + 2G\cos\theta)\delta\hat{q} + (\Delta + 2G\sin\theta)\delta\hat{p} + g\sin\psi\,\delta\hat{\phi} + \sqrt{\eta_c\kappa}\,\delta\hat{q}^{\text{in}} + \sqrt{(1-\eta_c)\kappa}\,\delta\hat{q}^0,$$
$$\delta\dot{\hat{p}} = -(\kappa/2 + 2G\cos\theta)\delta\hat{p} + (-\Delta + 2G\sin\theta)\delta\hat{q} - g\cos\psi\,\delta\hat{\phi} + \sqrt{\eta_c\kappa}\,\delta\hat{p}^{\text{in}} + \sqrt{(1-\eta_c)\kappa}\,\delta\hat{p}^0,$$
$$\delta\dot{\hat{\phi}} = \Omega_\phi\delta\hat{L}_z,$$
$$\delta\dot{\hat{L}}_z = -\Omega_\phi\delta\hat{\phi} - \Gamma_\tau\delta\hat{L}_z - g\cos\psi\,\delta\hat{q} - g\sin\psi\,\delta\hat{p} + \sqrt{2\Gamma_\tau}\,\hat{\tau}_{\text{in}}. \tag{5}$$

The effective COM coupling constant is $g = \sqrt{2}g_0|\alpha|$. According to Eq. (5), we use the flow chart in Fig. 2 to illustrate the flow of quantum backaction noise. In a conventional COM system, the radiation pressure force of photons acts on the phonons, introducing optomechanical backaction noise (Path ①). In the presence of intracavity squeezing, another backaction noise path from $\delta\hat{q}$ to $\delta\hat{p}$ emerges (Path ②). The destructive interference between the two noise channels results in a reduction of quantum backaction noise in the COM sensor, thereby increasing the sensitivity of torque sensing, as illustrated in Fig. 2.

To obtain information about the intracavity field, it is often necessary to measure the field that escapes the cavity, as direct measurement is typically difficult. Therefore, with help from the input-output relation $\hat{a}_{\text{out}} = \sqrt{\eta_c\kappa}\hat{a} - \hat{a}_{\text{in}}$ [11], the output quadrature fluctuations can be written as

$$\delta\hat{\mathbf{Q}}_{\text{out}}[\Omega] = \mathcal{L}[\Omega]\delta\hat{\mathbf{V}}_{\text{in}}[\Omega],$$

where

$$\hat{\mathbf{Q}}_{\text{out}}[\Omega] = (\hat{q}_{\text{out}} \quad \hat{p}_{\text{out}})^{\text{T}},$$
$$\hat{\mathbf{V}}_{\text{in}}[\Omega] = (\hat{q}_{\text{in}} \quad \hat{p}_{\text{in}} \quad \hat{q}_0 \quad \hat{p}_0 \quad \hat{\tau}_{\text{in}})^{\text{T}},$$
$$\mathcal{L}[\Omega] = \begin{pmatrix} \mathcal{C}_+ & \mathcal{D}_+ & \mathcal{A}_+ & \mathcal{B}_+ & \mathcal{N}_+ \\ \mathcal{A}_- & \mathcal{B}_- & \mathcal{C}_- & \mathcal{D}_- & \mathcal{N}_- \end{pmatrix}. \tag{6}$$

The coefficients can be obtained through straightforward algebraic manipulations as follows:

$$\mathcal{A}_\pm[\Omega] = \kappa\eta_c(\lambda_\pm^{-1} - \mu_+\mu_-\lambda_\mp)^{-1}\lambda_\mp\mu_\pm,$$
$$\mathcal{B}_\pm[\Omega] = \kappa\lambda_\mp\mu_\pm(\lambda_\pm^{-1} - \mu_+\mu_-\lambda_\mp)^{-1}\sqrt{\eta_c(1-\eta_c)},$$
$$\mathcal{C}_\pm[\Omega] = \kappa\eta_c(\lambda_\pm^{-1} - \mu_+\mu_-\lambda_\mp)^{-1} - 1,$$
$$\mathcal{D}_\pm[\Omega] = \kappa(\lambda_\pm^{-1} - \mu_+\mu_-\lambda_\mp)^{-1}\sqrt{\eta_c(1-\eta_c)},$$
$$\mathcal{N}_+[\Omega] = \frac{\sqrt{2\eta_c\kappa\Gamma_\tau}g\chi_\tau(\mu_+\lambda_-\cos\psi - \sin\psi)}{(\lambda_+^{-1} - \mu_+\mu_-\lambda_-)},$$
$$\mathcal{N}_-[\Omega] = \frac{\sqrt{2\eta_c\kappa\Gamma_\tau}g\chi_\tau(-\mu_-\lambda_+\sin\psi + \cos\psi)}{(\lambda_-^{-1} - \mu_+\mu_-\lambda_+)},$$

with

$$\mu_\pm[\Omega] = \mp\Delta + 2G\sin\theta - \tfrac{1}{2}g^2\chi_\tau[1 \pm \cos(2\psi)],$$
$$\lambda_\pm[\Omega] = \left[(\kappa/2 - i\Omega) \mp 2G\cos\theta \pm \tfrac{1}{2}g^2\chi_\tau\sin(2\psi)\right]^{-1},$$

and $\chi_\tau = \Omega_\phi/(\Omega_\phi^2 - \Omega^2 - i\Omega\Gamma_\tau)$ represents the mechanical susceptibility of the system [11].

Homodyne measurement allows one to read out the output spectrum by mixing the output field with a local oscillator at a 50:50 beam splitter [42]. Suppose the local oscillator has a phase φ, then the measured quadrature can be written as

$$\delta\hat{q}_{\text{out}}^\varphi[\Omega] = \delta\hat{q}_{\text{out}}\cos\varphi + \delta\hat{p}_{\text{out}}\sin\varphi. \tag{7}$$

We can present the expressions for the output amplitude quadrature spectrum and the output phase quadrature

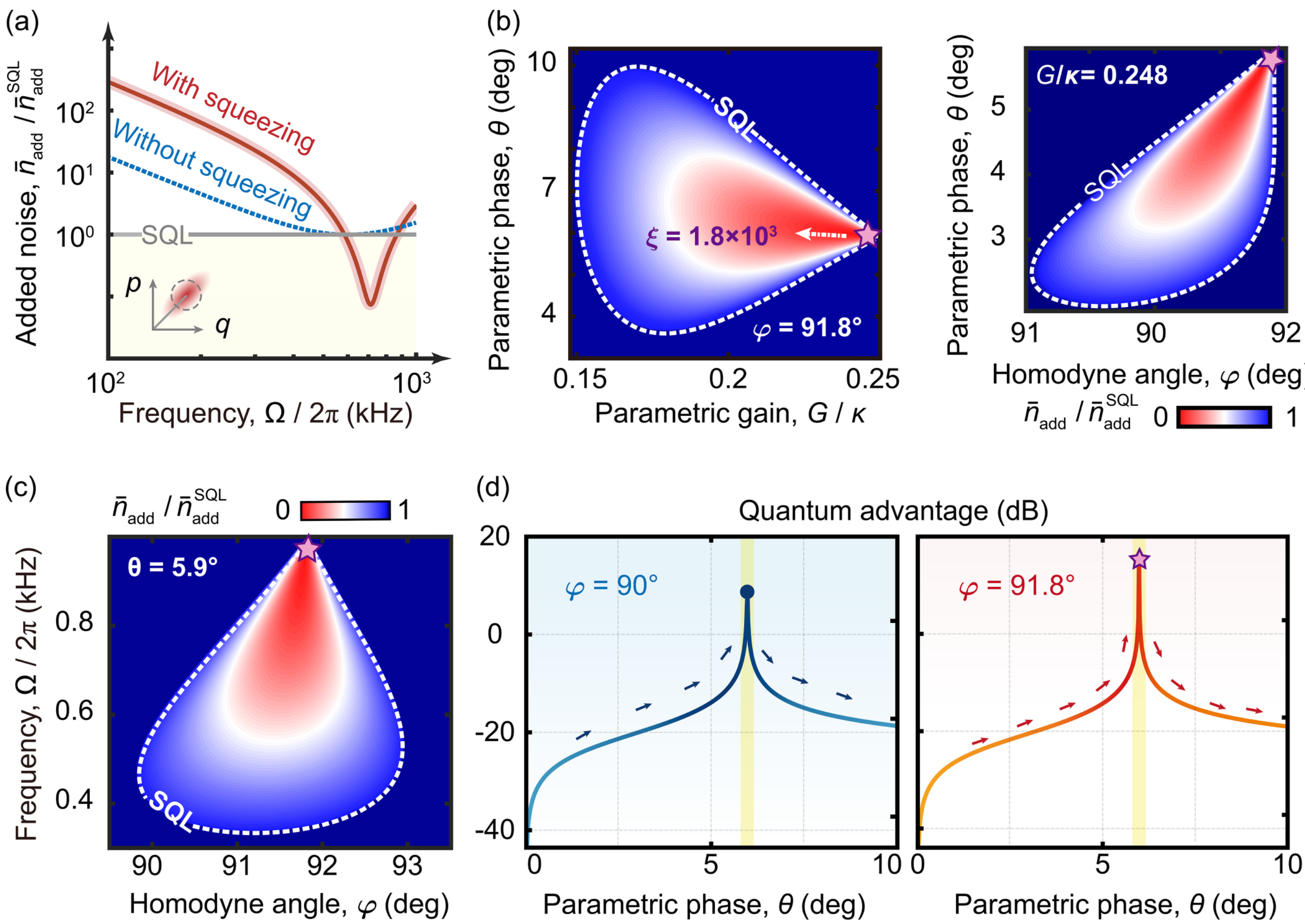

FIG. 3. (a) Added noise in the frequency domain is plotted with or without squeezing for standard phase detection. The gray solid line represents the SQL. (b) In the presence of squeezing, the added noise $\bar{n}_{\rm add}$ is significantly suppressed below the SQL. The scaled noise spectrum $\bar{n}_{\rm add}/\bar{n}_{\rm add}^{\rm SQL}$ versus the homodyne angle ϕ and the parametric phase θ. (c) The scaled noise spectrum $\bar{n}_{\rm add}/\bar{n}_{\rm add}^{\rm SQL}$ versus the phase of the homodyne angle ϕ and the Fourier frequency Ω. (d) For different homodyne angles, the quantum advantage is depicted versus the parametric phase θ. The remaining parameters are $G/\kappa = 0.248$, $\theta = 5.9^\circ$, and $\eta_c = 1$.

spectrum [42] as follows:

$$\begin{aligned}\bar{S}_{\rm qq}^{\rm out}[\Omega] &= \tfrac{1}{2}\langle\{\delta\hat{q}_{\rm out}[\Omega]\delta\hat{q}_{\rm out}[-\Omega]\}\rangle\\ &= \tfrac{1}{2}\mathcal{K}_+[\Omega] + \bar{n}_m|\mathcal{N}_+[\Omega]|^2,\\ \bar{S}_{\rm pp}^{\rm out}[\Omega] &= \tfrac{1}{2}\langle\{\delta\hat{p}_{\rm out}[\Omega]\delta\hat{p}_{\rm out}[-\Omega]\}\rangle\\ &= \tfrac{1}{2}\mathcal{K}_-[\Omega] + \bar{n}_m|\mathcal{N}_-[\Omega]|^2.\end{aligned} \tag{8}$$

The above equations include the following introduced definitions:

$$\begin{aligned}\mathcal{K}_+ &= |\mathcal{A}_+|^2 + |\mathcal{B}_+|^2 + |\mathcal{C}_+|^2 + |\mathcal{D}_+|^2,\\ \mathcal{K}_- &= |\mathcal{A}_-|^2 + |\mathcal{B}_-|^2 + |\mathcal{C}_-|^2 + |\mathcal{D}_-|^2,\end{aligned} \tag{9}$$

where $\mathcal{K}_+$ and $\mathcal{K}_-$ represent the effects of shot noise and backaction noise on the output amplitude quadrature spectrum $\bar{S}_{\rm qq}^{\rm out}$ and the output phase quadrature spectrum $\bar{S}_{\rm pp}^{\rm out}$, respectively. $\mathcal{N}_\pm$ denotes the noise imprinted by mechanical motion in these spectra. The symmetrized cross-correlation spectrum can then be written as

$$\begin{aligned}\bar{S}_{\rm pq}^{\rm out}[\Omega] &= \tfrac{1}{2}\langle\{\delta\hat{q}_{\rm out}[\Omega]\delta\hat{p}_{\rm out}[-\Omega]\}\rangle\\ &= {\rm Re}\big\{\tfrac{1}{2}(\mathcal{K}_{\rm cr}[\Omega] + i\mathcal{K}_{\rm si}[\Omega]) + \bar{n}_m\mathcal{N}[\Omega]\big\},\end{aligned} \tag{10}$$

where

$$\begin{aligned}\mathcal{K}_{\rm cr} &= \mathcal{C}_+\mathcal{A}_-^* + \mathcal{D}_+\mathcal{B}_-^* + \mathcal{A}_+\mathcal{C}_-^* + \mathcal{B}_+\mathcal{D}_-^*,\\ \mathcal{K}_{\rm si} &= \mathcal{C}_+\mathcal{C}_-^* + \mathcal{D}_+\mathcal{D}_-^* - \mathcal{A}_+\mathcal{A}_-^* - \mathcal{B}_+\mathcal{B}_-^*,\\ \mathcal{K}_{\rm co} &= \mathcal{K}_{\rm cr} + i\mathcal{K}_{\rm si}, \quad \mathcal{N} = \mathcal{N}_+^*\mathcal{N}_-.\end{aligned} \tag{11}$$

Here $\mathcal{K}_{\rm co}$ contains the correlations between shot noise and backaction noise. Thus, we can calculate the homodyne photocurrent spectrum and get

$$\begin{aligned}\bar{S}_{\rm II}[\Omega] &= \tfrac{1}{2}\big\langle\big\{\delta\hat{q}_{\rm out}^{\varphi}[\Omega]\delta\hat{q}_{\rm out}^{\varphi}[-\Omega]\big\}\big\rangle\\ &= \bar{S}_{\rm qq}^{\rm out}\cos^2\varphi + \bar{S}_{\rm pp}^{\rm out}\sin^2\varphi + \bar{S}_{\rm pq}^{\rm out}\sin(2\varphi)\\ &= \mathcal{R}_\tau[\Omega](\bar{n}_m + \bar{n}_{\rm add}[\Omega]).\end{aligned} \tag{12}$$

In the case of squeezing, by adjusting the squeezed parameters G and θ, the cross term $\mathcal{K}_{\rm co}$ in $\bar{S}_{\rm pq}^{\rm out}$ can become negative, allowing for the effective cancellation of backaction noise and shot noise. The mechanical response of such a COM torque sensor to the detected torque is given by

$$\mathcal{R}_\tau = |\mathcal{N}_+|^2 \cos^2\varphi + |\mathcal{N}_-|^2 \sin^2\varphi + \mathrm{Re}\mathcal{N}\sin(2\varphi), \quad (13)$$

and the added noise, described as

$$\bar{n}_{\mathrm{add}} = \frac{\mathcal{K}_+\cos^2\varphi + \mathcal{K}_-\sin^2\varphi + \mathrm{Re}\mathcal{K}_{\mathrm{cr}} + i\mathcal{K}_{\mathrm{si}}\sin(2\varphi)}{2\mathcal{R}_\tau}, \quad (14)$$

comprising two quantum noise sources, contributes to the spectrum of the total torque noise, which is crucial for estimating the sensitivity of torque measurements. We can determine the torque noise spectrum as

$$\bar{S}_{\tau\tau}[\Omega] = 2\hbar\Omega_\phi\Gamma_\tau I(\bar{n}_m + \bar{n}_{\mathrm{add}}[\Omega]). \quad (15)$$

In the following discussion, we subtract the effects of thermal noise and other sources of technical noise, focusing on the case of $\Delta = 0$ to reveal the influence of optical squeezing on the quantum-enhanced COM torque sensor.

To simplify the equations, we assume the limit $\kappa \gg \Omega$. Under this condition, the added noise in the torque sensing procedure without intracavity squeezing and with standard phase detection ($\phi = 90^\circ$) can be expressed in a simplified form:

$$\bar{n}_{\mathrm{add}} = \bar{n}_{\mathrm{add}}^{\mathrm{shot}} + \bar{n}_{\mathrm{add}}^{\mathrm{qba}} = \frac{g^2}{\kappa\Gamma_\tau} + \frac{1}{16}\frac{\kappa}{g^2\Gamma_\tau}\frac{1}{|\chi_\tau|^2}. \quad (16)$$

This equation illustrates a trade-off between shot noise and backaction noise in torque measurement, and the minimum added noise is given by

$$\bar{n}_{\mathrm{add}}^{\mathrm{SQL}}[\Omega] = \frac{1}{2\Gamma_\tau|\chi_\tau|}, \quad (17)$$

which is known as the SQL [11]. When the added noise is below the SQL, it signs that the measurement is reaching the quantum regime. Quantum squeezing, observable through homodyne detection, is a well-known resource that can effectively suppress quantum noise, thereby enhancing the performance of quantum sensors [26]. As depicted in Fig. 3(a), the added noise $\bar{n}_{\mathrm{add}}$ scaled by $\bar{n}_{\mathrm{add}}^{\mathrm{SQL}}$ is plotted as a function of Fourier frequency. We see that in the absence of intracavity squeezing, there is always $\bar{n}_{\mathrm{add}}/\bar{n}_{\mathrm{SQL}} > 1$, indicating that the torque sensitivity described in Eq. (15) is constrained by the SQL. When squeezing is applied, quantum noise can be suppressed well below the SQL. This suppression of noise can consequently enhance torque sensitivity [see Eq. (15)].

Quantum-enhanced torque measurement can be characterized by the enhancement factor resulting from the squeezing:

$$\xi = \frac{\min\{\bar{S}_\tau(G=0,\theta=0)\}}{\min\{\bar{S}_\tau(G\neq 0,\theta\neq 0)\}}. \quad (18)$$

Figure 3(b) illustrates the features of the scaled noise spectrum $\bar{n}_{\mathrm{add}}/\bar{n}_{\mathrm{add}}^{\mathrm{SQL}}$ in homodyne detection as a function of the homodyne angle φ and the parametric phase θ. At a fixed parameter gain G, the homodyne angle φ is optimized for each parametric phase θ set rather than considering the standard phase detection. To find the optimal sensitivity, we plot the scaled noise spectrum $\bar{n}_{\mathrm{add}}/\bar{n}_{\mathrm{add}}^{\mathrm{SQL}}$ as a function of the parametric gain, the parametric phase, the Fourier frequency Ω, and the homodyne angle φ [see Figs. 3(b) and 3(c)]. The plot demonstrates that the minimum added noise may be reduced by 3 orders of magnitude below the SQL when $G/\kappa = 0.248$, $\theta = 5.9^\circ$, $\Omega/2\pi = 1$ kHz, and $\varphi = 91.8^\circ$. A central goal of any quantum technology is to demonstrate a performance advantage over the best possible classical implementation. To explore the quantum advantage of this quantum squeezing-enhanced COM torque sensor compared to its classical counterparts, we define the following ratio as

$$\chi\ (\mathrm{dB}) = 10\log_{10}\sqrt{\frac{\bar{S}_\tau^{\mathrm{SQL}}[\Omega](G=0,\theta=0)}{\bar{S}_\tau[\Omega](G\neq 0,\theta\neq 0)}}, \quad (19)$$

where $\bar{S}_\tau^{\mathrm{SQL}}[\Omega]$ denotes the minimum added noise of the classical COM torque sensor [72]. Figure 3(d) shows this ratio as a function of θ, indicating that the quantum advantage is present when the ratio exceeds 0 dB. Clearly, the added noise imprinted on the torque-noise spectrum can be minimized by choosing an appropriate homodyne angle, which can further enhance the quantum advantage to an optimal value of about 20 dB, as shown in the right panel of Fig. 3(d). As depicted in Fig. 4, the advantage of our squeezing-enhanced COM torque sensor diminishes significantly as thermal noise increases. However, even at finite temperatures, the torque sensitivity of the squeezing-enhanced COM torque sensor remains superior to that of the SQL. Based on the above analysis, in practical applications, when dilution refrigeration or other cooling

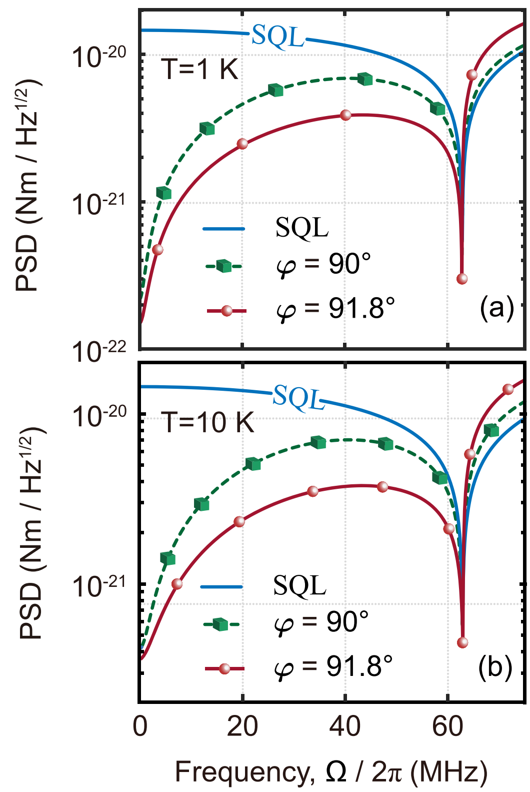

FIG. 4. (a) and (b) The power spectral density (PSD) in the presence of thermal noise. The blue curve corresponds to the SQL. By considering intracavity squeezing with parameters $G/\kappa = 0.248$ and $\theta = 5.9^\circ$, a detection angle of $\varphi = 91.8^\circ$ (red curve) optimizes sensitivity compared to standard phase detection (green curve).

technologies have effectively minimized the thermal noise of the system [73,74], further improvements can be achieved by incorporating feedback-controlled in-loop light and the injection of squeezed light [37,38,75].

III. CONCLUSIONS

In conclusion, our study focuses on investigating the influence of quantum squeezing, which is induced by quantum correlations between optical quadratures, on COM torque sensing. Our findings demonstrate that the performance of COM torque sensors can be significantly improved by effectively suppressing quantum noise, achieving 3 orders of magnitude less noise than the SQL. We expect that combining it with other existing techniques of fabricating and operating COM-based sensors, such as those involving feedback control [13,76] or advanced materials with much higher mechanical Q factors [77,78], can further improve performance in practice. It is our hope that these results will stimulate further efforts toward building and utilizing quantum-squeezing-enhanced torque sensors, such as those based on levitated spheres [79,80], solid-state mechanical devices [27,81–83], and nonreciprocal systems [84–91], to realize high-precision accelerometers or gyroscopes [92,93] and torsional magnetometry [94–96].

ACKNOWLEDGMENTS

H.J. is supported by the National Natural Science Foundation of China (Grant No. 11935006), the Science and Technology Innovation Program of Hunan Province (Grant No. 2020RC4047), the National Key R&D Program of China (Grant No. 2024YFE0102400), and the Hunan provincial major sci-tech program (Grant No. 2023ZJ1010).

[1] R. A. Beth, Mechanical detection and measurement of the angular momentum of light, Phys. Rev. **50**, 115 (1936).

[2] E. Brasselet, Torsion pendulum driven by the angular momentum of light: Beth's legacy continues, Adv. Photon. **5**, 034003 (2023).

[3] H. B. Chan, V. A. Aksyuk, R. N. Kleiman, D. J. Bishop, and F. Capasso, Quantum mechanical actuation of microelectromechanical systems by the Casimir force, Science **291**, 1941 (2001).

[4] Z. Xu and T. Li, Detecting Casimir torque with an optically levitated nanorod, Phys. Rev. A **96**, 033843 (2017).

[5] D. A. T. Somers, J. L. Garrett, K. J. Palm, and J. N. Munday, Measurement of the Casimir torque, Nature (London) **564**, 386 (2018).

[6] G. G. Luther and W. R. Towler, Redetermination of the Newtonian gravitational constant *g*, Phys. Rev. Lett. **48**, 121 (1982).

[7] H. Cavendish, Experiments to determine the density of the earth, Philos. Trans. R. Soc. Lond. **88**, 469 (1798).

[8] D. Rugar, R. Budakian, H. J. Mamin, and B. W. Chui, Single spin detection by magnetic resonance force microscopy, Nature (London) **430**, 329 (2004).

[9] J. P. Davis, D. Vick, J. A. J. Burgess, D. C. Fortin, P. Li, V. Sauer, W. K. Hiebert, and M. R. Freeman, Observation of magnetic supercooling of the transition to the vortex state, New J. Phys. **12**, 093033 (2010).

[10] M. M. van Oene, L. E. Dickinson, F. Pedaci, M. Köber, D. Dulin, J. Lipfert, and N. H. Dekker, Biological magnetometry: Torque on superparamagnetic beads in magnetic fields, Phys. Rev. Lett. **114**, 218301 (2015).

[11] M. Aspelmeyer, T. J. Kippenberg, and F. Marquardt, Cavity optomechanics, Rev. Mod. Phys. **86**, 1391 (2014).

[12] B.-B. Li, L. Ou, Y. Lei, and Y.-C. Liu, Cavity optomechanical sensing, Nanophotonics **10**, 2799 (2021).

[13] E. Gavartin, P. Verlot, and T. J. Kippenberg, A hybrid on-chip optomechanical transducer for ultrasensitive force measurements, Nat. Nanotechnol. **7**, 509 (2012).

[14] M. Tse *et al.*, Quantum-enhanced advanced LIGO detectors in the era of gravitational-wave astronomy, Phys. Rev. Lett. **123**, 231107 (2019).

[15] M. J. Yap *et al.*, Broadband reduction of quantum radiation pressure noise via squeezed light injection, Nat. Photon. **14**, 19 (2020).

[16] M. Wu, A. C. Hryciw, C. Healey, D. P. Lake, H. Jayakumar, M. R. Freeman, J. P. Davis, and P. E. Barclay, Dissipative and dispersive optomechanics in a nanocavity torque sensor, Phys. Rev. X **4**, 021052 (2014).

[17] H. Kaviani, B. Behera, G. Hajisalem, G. de Oliveira Luiz, D. P. Lake, and P. E. Barclay, High-frequency torsional motion transduction using optomechanical coupled oscillators, Optica **10**, 35 (2023).

[18] H. Zhang, M. Peng, X.-W. Xu, and H. Jing, Anti-symmetric Kerr gyroscope, Chin. Phys. B **31**, 014215 (2022).

[19] M. Wu, N. L. Y. Wu, T. Firdous, F. Fani Sani, J. E. Losby, M. R. Freeman, and P. E. Barclay, Nanocavity optomechanical torque magnetometry and radiofrequency susceptometry, Nat. Commun. **12**, 127 (2017).

[20] P. H. Kim, B. D. Hauer, T. J. Clark, F. Fani Sani, M. R. Freeman, and J. P. Davis, Magnetic actuation and feedback cooling of a cavity optomechanical torque sensor, Nat. Commun. **8**, 1355 (2017).

[21] P. H. Kim, B. D. Hauer, C. Doolin, F. Souris, and J. P. Davis, Approaching the standard quantum limit of mechanical torque sensing, Nat. Commun. **7**, 13165 (2016).

[22] L. He, H. Li, and M. Li, Optomechanical measurement of photon spin angular momentum and optical torque in integrated photonic devices, Sci. Adv. **2**, e1600485 (2016).

[23] H. Kaviani, R. Ghobadi, B. Behera, M. Wu, A. Hryciw, S. Vo, D. Fattal, and P. Barclay, Optomechanical detection of light with orbital angular momentum, Opt. Express **28**, 15482 (2020).

[24] M. Bhattacharya, P.-L. Giscard, and P. Meystre, Entanglement of a Laguerre-Gaussian cavity mode with a rotating mirror, Phys. Rev. A **77**, 013827 (2008).

[25] A. A. Clerk, M. H. Devoret, S. M. Girvin, F. Marquardt, and R. J. Schoelkopf, Introduction to quantum noise, measurement, and amplification, Rev. Mod. Phys. **82**, 1155 (2010).

[26] B. J. Lawrie, P. D. Lett, A. M. Marino, and R. C. Pooser, Quantum sensing with squeezed light, ACS Photon. **6**, 1307 (2019).

[27] K. A. Gilmore, M. Affolter, R. J. Lewis-Swan, D. Barberena, E. Jordan, A. M. Rey, and J. J. Bollinger, Quantum-enhanced sensing of displacements and electric fields with two-dimensional trapped-ion crystals, Science **373**, 673 (2021).

[28] D. Mason, J. Chen, M. Rossi, Y. Tsaturyan, and A. Schliesser, Continuous force and displacement measurement below the standard quantum limit, Nat. Phys. **15**, 745 (2019).

[29] J. Wang, Q. Zhang, Y.-F. Jiao, S.-D. Zhang, T.-X. Lu, Z. Li, C.-W. Qiu, and H. Jing, Quantum advantage of one-way squeezing in weak-force sensing, Appl. Phys. Rev. **11**, 031409 (2024).

[30] Q. Zhang, J. Wang, T.-X. Lu, R. Huang, F. Nori, and H. Jing, Quantum weak force sensing with squeezed magnomechanics, Sci. China Phys. Mech. Astron. **67**, 100313 (2024).

[31] A. Mehmood, S. Qamar, and S. Qamar, Effects of laser phase fluctuation on force sensing for a free particle in a dissipative optomechanical system, Phys. Rev. A **98**, 053841 (2018).

[32] C. D. Aiello, M. Hirose, and P. Cappellaro, Composite-pulse magnetometry with a solid-state quantum sensor, Nat. Commun. **4**, 1419 (2013).

[33] C. Troullinou, V. G. Lucivero, and M. W. Mitchell, Quantum-enhanced magnetometry at optimal number density, Phys. Rev. Lett. **131**, 133602 (2023).

[34] G.-L. Zhu, J. Liu, Y. Wu, and X.-Y. Lü, Quantum magnetometer with dual-coupling optomechanics, Laser Photon. Rev. **16**, 2100636 (2022).

[35] M. Metcalfe, Applications of cavity optomechanics, Appl. Phys. Rev. **1**, 031105 (2014).

[36] S. Barzanjeh, A. Xuereb, S. Gröblacher, M. Paternostro, C. A. Regal, and E. M. Weig, Optomechanics for quantum technologies, Nat. Phys. **18**, 15 (2022).

[37] X.-Y. Lü, Y. Wu, J. R. Johansson, H. Jing, J. Zhang, and F. Nori, Squeezed optomechanics with phase-matched amplification and dissipation, Phys. Rev. Lett. **114**, 093602 (2015).

[38] W. Qin, A. Miranowicz, P.-B. Li, X.-Y. Lü, J. Q. You, and F. Nori, Exponentially enhanced light-matter interaction, cooperativities, and steady-state entanglement using parametric amplification, Phys. Rev. Lett. **120**, 093601 (2018).

[39] N. S. Kampel, R. W. Peterson, R. Fischer, P.-L. Yu, K. Cicak, R. W. Simmonds, K. W. Lehnert, and C. A. Regal, Improving broadband displacement detection with quantum correlations, Phys. Rev. X **7**, 021008 (2017).

[40] Y. Xia, A. R. Agrawal, C. M. Pluchar, A. J. Brady, Z. Liu, Q. Zhuang, D. J. Wilson, and Z. Zhang, Entanglement-enhanced optomechanical sensing, Nat. Photon. **17**, 470 (2023).

[41] H. Yu *et al.*, Quantum correlations between light and the kilogram-mass mirrors of LIGO, Nature (London) **583**, 43 (2020).

[42] V. Sudhir, R. Schilling, S. A. Fedorov, H. Schutz, D. J. Wilson, and T. J. Kippenberg, Quantum correlations of light from a room-temperature mechanical oscillator, Phys. Rev. X **7**, 031055 (2017).

[43] M. Tsang and C. M. Caves, Evading quantum mechanics: Engineering a classical subsystem within a quantum environment, Phys. Rev. X **2**, 031016 (2012).

[44] C. B. Møller, R. A. Thomas, G. Vasilakis, E. Zeuthen, Y. Tsaturyan, M. Balabas, K. Jensen, A. Schliesser, K. Hammerer, and E. S. Polzik, Quantum back-action-evading measurement of motion in a negative mass reference frame, Nature (London) **547**, 191 (2017).

[45] L. M. de Lépinay, C. F. Ockeloen-Korppi, M. J. Woolley, and M. A. Sillanpää, Quantum mechanics-free subsystem with mechanical oscillators, Science **372**, 625 (2021).

[46] H. Li and M. Li, Optomechanical photon shuttling between photonic cavities, Nat. Nanotechnol. **9**, 913 (2014).

[47] J. Ahn, Z. Xu, J. Bang, P. Ju, X. Gao, and T. Li, Ultrasensitive torque detection with an optically levitated nanorotor, Nat. Nanotechnol. **15**, 89 (2020).

[48] P.-B. Li, Y. Zhou, W.-B. Gao, and F. Nori, Enhancing spin-phonon and spin-spin interactions using linear resources in a hybrid quantum system, Phys. Rev. Lett. **125**, 153602 (2020).

[49] S. Zeytinoğlu, A. İmamoğlu, and S. Huber, Engineering matter interactions using squeezed vacuum, Phys. Rev. X **7**, 021041 (2017).

[50] S. C. Burd, R. Srinivas, H. M. Knaack, W. Ge, A. C. Wilson, D. J. Wineland, D. Leibfried, J. J. Bollinger, D. Allcock, and D. Slichter, Quantum amplification of boson-mediated interactions, Nat. Phys. **17**, 898 (2021).

[51] W. Qin, A. Miranowicz, H. Jing, and F. Nori, Generating long-lived macroscopically distinct superposition states in atomic ensembles, Phys. Rev. Lett. **127**, 093602 (2021).

[52] A. Kowalewska-Kudłaszyk, S. I. Abo, G. Chimczak, J. Peřina, F. Nori, and A. Miranowicz, Two-photon blockade and photon-induced tunneling generated by squeezing, Phys. Rev. A **100**, 053857 (2019).

[53] P. Groszkowski, H.-K. Lau, C. Leroux, L. C. G. Govia, and A. A. Clerk, Heisenberg-limited spin squeezing via bosonic parametric driving, Phys. Rev. Lett. **125**, 203601 (2020).

[54] Y.-H. Chen, W. Qin, X. Wang, A. Miranowicz, and F. Nori, Shortcuts to adiabaticity for the quantum Rabi model: Efficient generation of giant entangled cat states via parametric amplification, Phys. Rev. Lett. **126**, 023602 (2021).

[55] L. Tang, J. Tang, M. Chen, F. Nori, M. Xiao, and K. Xia, Quantum squeezing induced optical nonreciprocity, Phys. Rev. Lett. **128**, 083604 (2022).

[56] T.-X. Lu, Y. Wang, K. Xia, X. Xiao, L.-M. Kuang, and H. Jing, Quantum squeezing induced nonreciprocal phonon laser, Sci. China Phys. Mech. Astron. **67**, 260312 (2024).

[57] Y.-M. Liu, C.-H. Bai, D.-Y. Wang, T. Wang, M.-H. Zheng, H.-F. Wang, A.-D. Zhu, and S. Zhang, Ground-state cooling of rotating mirror in double-Laguerre-Gaussian-cavity with atomic ensemble, Opt. Express **26**, 6143 (2018).

[58] M. Bhattacharya and P. Meystre, Using a Laguerre-Gaussian beam to trap and cool the rotational motion of a mirror, Phys. Rev. Lett. **99**, 153603 (2007).

[59] D. Wei, P. Chen, Y. Zhang, W. Yao, R. Ni, X. Hu, X. Lv, S. Zhu, M. Xiao, and Y. Zhang, Generation of high-efficiency, high-purity, and broadband Laguerre-Gaussian modes from a Janus optical parametric oscillator, Adv. Photon. Nexus **2**, 036007 (2023).

[60] G. A. Phelps and P. Meystre, Laser phase noise effects on the dynamics of optomechanical resonators, Phys. Rev. A **83**, 063838 (2011).

[61] M. Abdi, S. Barzanjeh, P. Tombesi, and D. Vitali, Effect of phase noise on the generation of stationary entanglement in cavity optomechanics, Phys. Rev. A **84**, 032325 (2011).

[62] S. Qamar, H. Xiong, and M. S. Zubairy, Influence of pump-phase fluctuations on entanglement generation using a correlated spontaneous-emission laser, Phys. Rev. A **75**, 062305 (2007).

[63] A. Pontin, C. Biancofiore, E. Serra, A. Borrielli, F. S. Cataliotti, F. Marino, G. A. Prodi, M. Bonaldi, F. Marin, and D. Vitali, Frequency-noise cancellation in optomechanical systems for ponderomotive squeezing, Phys. Rev. A **89**, 033810 (2014).
[64] R. Ahmed and S. Qamar, Effects of laser phase noise on optomechanical entanglement in the presence of a nonlinear Kerr downconverter, Phys. Scr. **94**, 085102 (2019).
[65] A. Mehmood, S. Qamar, and S. Qamar, Force sensing in a dissipative optomechanical system in the presence of parametric amplifier's pump phase noise, Phys. Scr. **94**, 095502 (2019).
[66] Y. Zeng, B. Xiong, and C. Li, Suppressing laser phase noise in an optomechanical system, Front. Phys. **17**, 12503 (2022).
[67] W. Gu, Y. Wang, Z. Yi, W. Yang, and L. Sun, Force measurement in squeezed dissipative optomechanics in the presence of laser phase noise, Opt. Express **28**, 12460 (2020).
[68] M. Parniak, I. Galinskiy, T. Zwettler, and E. S. Polzik, High-frequency broadband laser phase noise cancellation using a delay line, Opt. Express **29**, 6935 (2021).
[69] W. Zhao, S.-D. Zhang, A. Miranowicz, and H. Jing, Weak-force sensing with squeezed optomechanics, Sci. China Phys. Mech. Astron. **63**, 224211 (2020).
[70] M. H. Wimmer, D. Steinmeyer, K. Hammerer, and M. Heurs, Coherent cancellation of backaction noise in optomechanical force measurements, Phys. Rev. A **89**, 053836 (2014).
[71] W. P. Bowen and G. J. Milburn, *Quantum Optomechanics* (CRC, Boca Raton, FL, 2015).
[72] F. Li, T. Li, M. O. Scully, and G. S. Agarwal, Quantum advantage with seeded squeezed light for absorption measurement, Phys. Rev. Appl. **15**, 044030 (2021).
[73] F. Fogliano, B. Besga, A. Reigue, L. Mercier de Lépinay, P. Heringlake, C. Gouriou, E. Eyraud, W. Wernsdorfer, B. Pigeau, and O. Arcizet, Ultrasensitive nano-optomechanical force sensor operated at dilution temperatures, Nat. Commun. **12**, 4124 (2021).
[74] I. Galinskiy, Y. Tsaturyan, M. Parniak, and E. S. Polzik, Phonon counting thermometry of an ultracoherent membrane resonator near its motional ground state, Optica **7**, 718 (2020).
[75] F. Bemani, O. Černotík, L. Ruppert, D. Vitali, and R. Filip, Force sensing in an optomechanical system with feedback-controlled in-loop light, Phys. Rev. Appl. **17**, 034020 (2022).
[76] G. I. Harris, D. L. McAuslan, T. M. Stace, A. C. Doherty, and W. P. Bowen, Minimum requirements for feedback enhanced force sensing, Phys. Rev. Lett. **111**, 103603 (2013).
[77] M. J. Bereyhi, A. Beccari, R. Groth, S. A. Fedorov, A. Arabmoheghi, T. J. Kippenberg, and N. J. Engelsen, Hierarchical tensile structures with ultralow mechanical dissipation, Nat. Commun. **13**, 3097 (2022).
[78] A. Beccari, D. A. Visani, S. A. Fedorov, M. J. Bereyhi, V. Boureau, N. J. Engelsen, and T. J. Kippenberg, Strained crystalline nanomechanical resonators with quality factors above 10 billion, Nat. Phys. **18**, 436 (2022).
[79] T. M. Hoang, Y. Ma, J. Ahn, J. Bang, F. Robicheaux, Z.-Q. Yin, and T. Li, Torsional optomechanics of a levitated nonspherical nanoparticle, Phys. Rev. Lett. **117**, 123604 (2016).
[80] N. P. Bullier, A. Pontin, and P. F. Barker, Quadratic optomechanical cooling of a cavity-levitated nanosphere, Phys. Rev. Res. **3**, L032022 (2021).
[81] X.-D. Chen, E.-H. Wang, L.-K. Shan, S.-C. Zhang, C. Feng, Y. Zheng, Y. Dong, G.-C. Guo, and F.-W. Sun, Quantum enhanced radio detection and ranging with solid spins, Nat. Commun. **14**, 1288 (2023).
[82] Y.-F. Jiao, Y.-L. Zuo, Y. Wang, W. Lu, J.-Q. Liao, L.-M. Kuang, and H. Jing, Tripartite quantum entanglement with squeezed optomechanics, Laser Photon. Rev., 2301154 (2024).
[83] S.-D. Zhang, J. Wang, Q. Zhang, Y.-F. Jiao, Y.-L. Zuo, Ş. K. Özdemir, C.-W. Qiu, F. Nori, and H. Jing, Squeezing-enhanced quantum sensing with quadratic optomechanics, Opt. Quantum **2**, 222 (2024).
[84] K. Xia, F. Nori, and M. Xiao, Cavity-free optical isolators and circulators using a chiral cross-Kerr nonlinearity, Phys. Rev. Lett. **121**, 203602 (2018).
[85] P. Yang, M. Li, X. Han, H. He, G. Li, C.-L. Zou, P. Zhang, Y. Qian, and T. Zhang, Non-reciprocal cavity polariton with atoms strongly coupled to optical cavity, Laser Photon. Rev. **17**, 2200574 (2023).
[86] X. Lu, W. Cao, W. Yi, H. Shen, and Y. Xiao, Nonreciprocity and quantum correlations of light transport in hot atoms via reservoir engineering, Phys. Rev. Lett. **126**, 223603 (2021).
[87] S. Yu, Y. Meng, J.-S. Tang, X.-Y. Xu, Y.-T. Wang, P. Yin, Z.-J. Ke, W. Liu, Z.-P. Li, Y.-Z. Yang, G. Chen, Y.-J. Han, C.-F. Li, and G.-C. Guo, Experimental investigation of quantum $\mathcal{PT}$-enhanced sensor, Phys. Rev. Lett. **125**, 240506 (2020).
[88] M. Zhang, W. Sweeney, C. W. Hsu, L. Yang, A. D. Stone, and L. Jiang, Quantum noise theory of exceptional point amplifying sensors, Phys. Rev. Lett. **123**, 180501 (2019).
[89] C. Wang, Z. Fu, W. Mao, J. Qie, A. D. Stone, and L. Yang, Non-Hermitian optics and photonics: From classical to quantum, Adv. Opt. Photon. **15**, 442 (2023).
[90] W. Ding, X. Wang, and S. Chen, Fundamental sensitivity limits for non-Hermitian quantum sensors, Phys. Rev. Lett. **131**, 160801 (2023).
[91] A. Graf, S. D. Rogers, J. Staffa, U. A. Javid, D. H. Griffith, and Q. Lin, Nonreciprocity in photon pair correlations of classically reciprocal systems, Phys. Rev. Lett. **128**, 213605 (2022).
[92] X. Mao, H. Yang, D. Long, M. Wang, P.-Y. Wen, Y.-Q. Hu, B.-Y. Wang, G.-Q. Li, J.-C. Gao, and G.-L. Long, Experimental demonstration of mode-matching and Sagnac effect in a millimeter-scale wedged resonator gyroscope, Photon. Res. **10**, 2115 (2022).
[93] K. Liu, C. Cai, J. Li, L. Ma, H. Sun, and J. Gao, Squeezing-enhanced rotating-angle measurement beyond the quantum limit, Appl. Phys. Lett. **113**, 261103 (2018).
[94] J. P. Davis, D. Vick, D. C. Fortin, J. A. J. Burgess, W. K. Hiebert, and M. R. Freeman, Nanotorsional resonator torque magnetometry, Appl. Phys. Lett. **96**, 072513 (2010).
[95] J. E. Losby, F. F. Sani, D. T. Grandmont, Z. Diao, M. Belov, J. A. J. Burgess, S. R. Compton, W. K. Hiebert, D. Vick, K. Mohammad, E. Salimi, G. E. Bridges, D. J. Thomson, and M. R. Freeman, Torque-mixing magnetic resonance spectroscopy, Science **350**, 798 (2015).
[96] Y. Wang, Z. Xiong, W.and Xu, G.-Q. Zhang, and J.-Q. You, Dissipation-induced nonreciprocal magnon blockade in a magnon-based hybrid system, Sci. China Phys. Mech. Astron. **65**, 260314 (2022).